Biofouling
Vol. 00, No. 0, Month 2008, 1–10

Taylor & Francis
Taylor & Francis Group

Surface-immobilised antimicrobial peptoids

Andrea R. Statz[a], Jong Pil Park[b], Nathaniel P. Chongsiriwatana[b], Annelise E. Barron[b,c,d] and Phillip B. Messersmith[a,c,e]*

[a]*Department of Biomedical Engineering, Northwestern University, Evanston, IL, USA;* [b]*Department of Chemical and Biological Engineering, Northwestern University, Evanston, IL, USA;* [c]*Institute for Bionanotechnology in Medicine, Northwestern University, Evanston, IL, USA;* [d]*Department of Bioengineering, Stanford University, Stanford, USA;* [e]*Department of Materials Science and Engineering, Northwestern University, Evanston, IL, USA*

(*Received 15 April 2008; final version received 19 June 2008*)

Surface modification techniques that create surfaces capable of killing adherent bacteria are promising solutions to infections associated with implantable medical devices. Antimicrobial (AMB) peptoid oligomers (ampetoids) that were designed to mimic helical AMB peptides were synthesised with a peptoid spacer chain to allow mobility and an adhesive peptide moiety for easy and robust immobilisation onto substrata. TiO_2 substrata were modified with the ampetoids and subsequently backfilled with an antifouling (AF) polypeptoid polymer in order to create polymer surface coatings composed of both AMB (active) and AF (passive) peptoid functionalities. Confocal microscopy images showed that the membranes of adherent *E. coli* cells were damaged after 2-h exposure to the modified substrata, suggesting that ampetoids retain AMB properties even when immobilised on substrata.

Keywords: ampetoids; antibacterial; antimicrobial; polypeptoid; antifouling

Introduction

Potential applications of surface-immobilised antimicrobial (AMB) polymers include medical devices, water purification systems, food packaging and hospital equipment (Kenawy et al. 2007). Bacterial infections on implanted medical devices such as catheters and pacemakers can lead to serious complications and, often, device removal because the adherent bacteria can form a biofilm, which provides a protective environment for bacteria against antibiotics and immune responses (Costerton et al. 1999; Habash and Reid 1999).

Strategies to limit bacterial fouling of surfaces can incorporate either passive or active elements. Passive approaches to fouling prevention lack an active antibacterial (ABT) component and typically involve the use of antifouling (AF) polymer surface coatings to provide steric resistance to physical attachment of bacteria. Examples of polymers that have been shown to reduce short-term bacterial attachment include poly(ethylene glycol) (PEG) (Kingshott et al. 2003; Harbers et al. 2007), self-assembled monolayers (SAMs) (Chapman et al. 2001), and peptide mimetic polymers (Statz et al. 2008).

Surface coatings may also contain active components capable of killing bacteria through direct contact or via a leachable compound. Examples of active AMB coatings include cationic polymers such as chitosan (Huh et al. 2001; Fu et al. 2005) and polymers containing quaternary ammonium (Lee et al. 2004; Cheng et al. 2005; Murata et al. 2007) and pyridinium (Tiller et al. 2001, 2002; Cen et al. 2004; Krishnan et al. 2006) functional groups. The ABT effect of silver can be exploited by incorporation of silver salts or silver nanoparticles into coatings (Sambhy et al. 2006; Marini et al. 2007; Ramstedt et al. 2007a,b). Another reported approach for creating ABT surfaces involves the direct attachment of antibiotics such as vancomycin (Jose et al. 2005) and penicillin (Aumsuwan et al. 2007) to surfaces. AMB peptides (AMPs) offer activity against a wide range of organisms, while functioning with some selectivity for bacteria over mammalian cells (Hancock and Sahl 2006), and there have been recent reports of AMP immobilisation onto surfaces (Appendini and Hotchkiss 2001; Gabriel et al. 2006).

Several non-natural mimics of AMPs with high activity have recently been developed, providing advantages in terms of chemical diversity and significant resistance to protease degradation (Miller et al. 1995). For example, the linear cationic α-helical class of AMPs has been successfully mimicked as *β*-peptides and as poly-*N*-substituted glycines (peptoids) (Porter et al. 2002; Patch and Barron 2003; Chongsiriwatana et al. 2008). Peptoids are non-natural mimics of polypeptides with the side chains appended to the amide nitrogen instead of the α-carbon

*Corresponding author. Email: philm@northwestern.edu

ISSN 0892-7014 print/ISSN 1029-2454 online

DOI: 10.1080/08927010802331829
http://www.informaworld.com

(Zuckermann et al. 1992). Peptoids are well suited for AMP use because they have been shown to be resistant to protease enzymes (Miller et al. 1995; Statz et al. 2008), the submonomer synthesis method allows for a great versatility of side-chain chemistry (Zuckermann et al. 1992), and helical secondary structures can be formed by incorporating bulky α-chiral side chains (Wu et al. 2001, 2003; Sanborn et al. 2002). Peptoid mimics of AMPs (ampetoids) with helical structures that exhibit ABT activity in solution have been synthesised previously (Patch and Barron 2003; Chongsiriwatana et al. 2008). Several ampetoids were recently tested for broad-spectrum activity and cytotoxicity, revealing peptoid sequences with ABT activity equivalent to cationic AMB peptides and with strong selectivity for bacteria over mammalian cells (Chongsiriwatana et al. 2008).

Peptoids can also offer passive resistance to biofouling, much like other AF polymers, as was first established with surfaces coated with a linear poly(*N*-methoxyethyl glycine) peptoid (Statz et al. 2005). Protein and cell adhesion on TiO_2 were substantially reduced by coating with this peptoid, which has side-chains similar to the repeat unit of PEG. A follow-up study revealed a substantial reduction in *Staphylococcus epidermidis* and *E. coli* adhesion when compared with unmodified TiO_2 substrata (Statz et al. 2008), presumably due to passive inhibition of bacterial cell attachment. In the current study, the passive resistance of *N*-methoxyethyl glycine peptoids was combined with an active AMP sequence identified in a previous ampetoid study (Chongsiriwatana et al. 2008). The results demonstrate a reduction in protein adsorption and fibroblast cell attachment. For surfaces incorporating the ABT peptoid sequence, a large fraction of the attached bacteria had compromised membranes, confirming that the immobilised ABT peptoid remained active.

Materials and methods

Materials

The primary amines for peptoid synthesis, 2,2,2-trifluoroethylamine, (*S*)-(−)-1-phenylethylamine, (*S*)-(+)-*sec*-butylamine, methoxyethylamine and 1,4-diaminobutane were purchased from Aldrich (Milwaukee, WI). Dimethylformamide (DMF), diisopropylethylamine (DIPEA), acetonitrile, *N*-morpholinopropanesufonic acid (MOPS) buffer salt, 4-(2-hydroxyethyl)piperazine-1-ethanesulfonic acid (HEPES) buffer salt, 2-propanol, 1,1′-dioctadecyl–3,3,3′,3′-tetramethylindocarbocyanine perchlorate (DiI) and fluorescein 5(6)-isothiocyanate (FITC) were also purchased from Aldrich (Milwaukee, WI). Rink amide MBHA resin was purchased from AnaSpec (San Jose, CA). Fmoc-Lys(Boc)-OH, Fmoc-Dopa(acetonide)-OH, and Fmoc-Pro-OH were purchased from Novabiochem (San Diego, CA). A protected submonomer (*N-tert*-butoxycarbonyl–1,4-butanediamine) was synthesised according to the published procedure (Krapcho and Kuell 1990), whereas all other primary amines for peptoid synthesis were used as purchased. Acetic anhydride, 2-(1H-benzotriazole-1-yl)- 1,1,3,3-tetramethylaminium hexafluorophosphate (HBTU), and *N*-methylpyrrolidone (NMP) were purchased from Applied Biosystems (Foster City, CA). Trifluoroacetic acid (TFA) was obtained from Acros Organics (Belgium). Silicon wafers were purchased from University Wafer (South Boston, MA). Glass microscope slides and Lab-tek two-well slide chambers were purchased from Fisher Scientific (Pittsburgh, PA). 3T3-Swiss albino fibroblasts, Dulbecco's modified Eagle's medium, foetal bovine serum, penicillin/streptomycin, trypsin-EDTA, and *E. coli* (ATCC 35218), *Bacillus subtilis* (ATCC 6633), *S. epidermidis* RP62A (ATCC 12228) and *Pseudomonas aeruginosa* (ATCC 700829) were obtained from American Type Culture Collection (Manassas, VA). Mueller–Hinton broth (MHB) and agar were purchased from Becton, Dickinson and Co. (Sparks, MD). Lyophilised whole human serum (Control Serum N) was purchased from Roche Diagnostics (Indianapolis, IN). The ultrapure water (UP H_2O) used for all experiments was purified (resistivity $\geq$ 18.2 MΩ-cm, total organic content $\leq$5 ppb) with a NANOpure Infinity System from Barnstead/Thermolyne Corporation (Dubuque, IA).

Synthesis

Polymer sequences and peptoid monomer side chains and amino acids are shown in Figure 1. Synthesis was performed on a C S Bio 036 (C S Bio, Menlo Park, CA) automated peptide synthesiser according to the previously described procedure (Statz et al. 2005). First, a *C-terminal* Dopa-Lys-Dopa-Lys-Dopa peptide was synthesised on rink amide MBHA resin using conventional Fmoc strategy of solid-phase peptide synthesis. This pentapeptide functions as an adhesive anchor for immobilisation of the peptoid onto surfaces (Statz et al. 2005). A 20-mer *N*-methoxyethyl glycine (*N*me) polypeptoid portion was then synthesised using a submonomer protocol (Zuckermann et al. 1992) and the resin was split. For PMP1-AMP and PMP1-C, submonomer synthesis was continued to add peptoid AMP (H-*N*Lys-*N*spe-*N*spe-*N*Lys-*N*spe-Pro-[*N*Lys-*N*spe-*N*spe]$_2$-NH_2) or peptoid C (H-[*N*Lys-*N*ssb-*N*ssb]$_4$-NH_2) (Chongsiriwatana et al. 2008), respectively, onto the N-terminus of the *N*me polypeptoid. During synthesis of PMP1-AMP and PMP1-C, a single residue of *N*-(2,2,2-trifluoroethyl) glycine (*N*tfe) was added between the peptide and peptoid fragments, as a label for X-ray photoelectron spectroscopy (XPS) compositional analysis.

PMP1-AMP
H-*N*Lys-*N*spe-*N*spe-*N*Lys-*N*spe-L-Pro-(*N*Lys-*N*spe-*N*spe)$_2$-(*N*me)$_{20}$-*N*tfe-(DOPA-Lys)$_2$-DOPA-NH$_2$

PMP1-C
H-(*N*Lys-*N*ssb-*N*ssb)$_4$-(*N*me)$_{20}$-*N*tfe-(DOPA-Lys)$_2$-DOPA-NH$_2$

PMP1$_{10}$
H-(*N*me)$_{10}$-(DOPA-Lys)$_2$-DOPA-NH$_2$

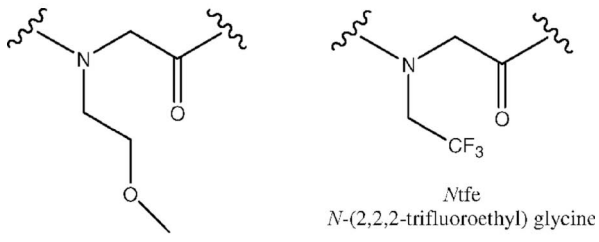

*N*me
N-methoxyethyl glycine

*N*tfe
N-(2,2,2-trifluoroethyl) glycine

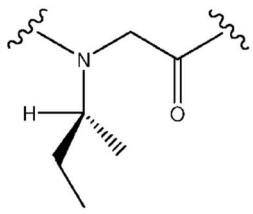

*N*ssb
(*S*)-*N*-(*sec*-butyl) glycine

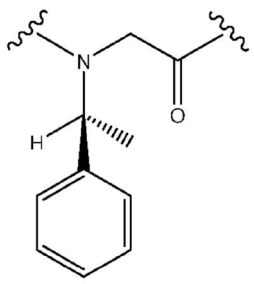

*N*spe
(*S*)-*N*-(1-phenylethyl) glycine

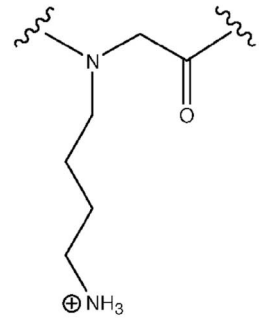

*N*Lys
N-(4-aminobutyl) glycine

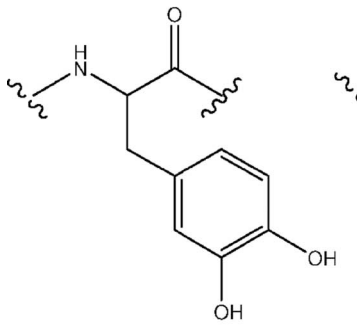

DOPA
3,4-dihydroxyphenylalanine

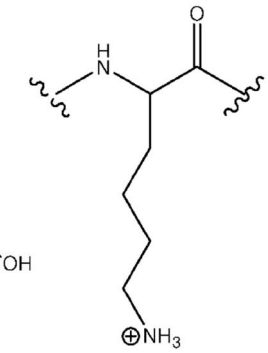

Lys
Lysine

Figure 1. Polymer sequences, peptoid monomer structures and amino acid structures with abbreviations.

PMP1$_{10}$ consisted of a 10-mer sequence of *N*me conjugated to the adhesive pentapeptide anchor, and was used as a passive 'backfilling' component in surfaces pre-adsorbed with PMP1-AMP.

Polymers were cleaved from the resin and the amino acid side-chains were deprotected by treating the resin with 95% (v/v) TFA, 2.5% H_2O and 2.5% TIS for 10 min, after which the cleaved polymer was removed by filtering and rinsing several times with TFA. Solvent was removed using a rotary evaporator; the product was dissolved in 50/50% water/acetonitrile, frozen and lyophilised. The crude products were purified by preparative reversed-phase high performance liquid chromatography (RP-HPLC) (Waters, Milford, MA) using a Vydac C18 column. The purity of each final product was confirmed by RP-HPLC and matrix-assisted laser desorption/ionisation mass spectrometry (MALDI-MS) (Voyager DE-Pro, Perspective Biosystem, MA).

ABT activity in solution

The minimum inhibitory concentration (MIC) for each polymer was determined according to the Clinical Laboratory Standards Institute (CLSI) broth microdilution protocols (M7-A6). The procedure explained previously was followed (Chongsiriwatana et al. 2008). Briefly, serial dilutions of the polymers were prepared in Mueller–Hinton broth (MHB) in 96-well microtiter plates, and bacterial inoculum in MHB was added to each well ($\sim 5.0 \times 10^4$ CFU well^{-1}). The optical density was monitored at 590 nm for 16 h at 35°C. The MIC was defined as the lowest concentration of peptoid/polymer necessary to completely inhibit bacterial growth for 16 h; experiments were repeated three times in duplicate for each bacterial strain including *E. coli, B. subtilis, S. epidermidis* and *P. aeruginosa*.

Circular dichroism spectroscopy

Circular dichroism (CD) measurements were conducted on a Jasco model 715 spectropolarimeter, using a quartz cylindrical cell (path length = 0.02 cm). Samples were dissolved at a concentration of 50 μM in 10 mM Tris-HCl (pH = 7.4). Scans were measured at 100 nm min^{-1} between 185 and 280 nm at 0.2 nm data pitch, 1 nm bandwidth, 2 s response and 100 mdeg sensitivity. The plots contain the average data from 40 spectral accumulations.

Surface modification

Silicon wafers and glass slides were coated with a 20-nm thick layer of TiO_2 by electron beam evaporation (Edwards Auto306; $<10^{-5}$ Torr) and the coated

wafers cut into 1-cm^2 pieces. The substrata were cleaned ultrasonically for 10 min in 2-propanol, dried under N_2, and then exposed to O_2 plasma (Harrick Scientific, Ossining, USA) at $\leq$150 Torr and 100 W for 3 min. Optical waveguide lightmode spectroscopy (OWLS) waveguides were purchased from MicroVacuum Ltd (Budapest, Hungary) (Voros et al. 2002) and coated with a 10-nm thick layer of TiO_2 by electron beam evaporation as described earlier. Sensors were cleaned following the same procedure as for the TiO_2 substrata. After use, OWLS waveguides were regenerated for subsequent use by 10-min sonication cycles in 0.1 M HCl, UP H_2O and 2-propanol followed by exposure to O_2 plasma to remove adsorbates.

Clean substrata and sensors were immersed in a 0.5 mg ml^{-1} solution of the appropriate ampetoid in UP H_2O at 25°C. After 2 h, substrata were removed and rinsed with UP H_2O to remove any unbound polymer, and then dried in a stream of filtered N_2. Next, the substrata were immersed in a 1.0 mg ml^{-1} solution of $PMP1_{10}$ in 3 M NaCl buffered with 0.1 M MOPS, pH = 6 (CP buffer) at 50°C for 6 h. After modification, substrata were extensively rinsed with UP H_2O to remove any unbound polymer, and then dried in a stream of filtered N_2.

XPS

Survey and high resolution XPS spectra were collected on an Omicron ESCALAB (Omicron, Taunusstein, Germany) configured with a monochromated Al Kα (1486.8 eV) 300-W X-ray source, 1.5 mm circular spot size, a flood gun to counter charging effects, and an ultrahigh vacuum ($<10^{-8}$ Torr). Substrata were prepared and analysed as previously described (Statz et al. 2008).

OWLS

OWLS was used to determine the optimum adsorption conditions for the polymers on TiO_2 surfaces. Clean TiO_2 sensors were inserted into the measurement head of an OWLS110 (MicroVacuum Ltd.) and exposed to the appropriate buffer solution through the flow-through cell (16 μl volume) for several hours to allow for equilibration. Ampetoid solutions were injected into the flow-through cell in stop-flow mode and allowed to adsorb for various times. The waveguide sensors were subsequently rinsed with buffer, and allowed to equilibrate for another 30 min. Between polymer adsorption steps, buffers were exchanged and the system was allowed to equilibrate for at least 10 h. The measured incoupling angles, α_{TM} and α_{TE} were converted to refractive indices N_{TM} and N_{TE} by the MicroVacuum software, and changes in refractive index at the sensor surface were converted to adsorbed mass using de Feijter's formula (de Feijter et al. 1978). The refractive indices of solutions were measured using a refractometer (J157 Automatic Refractometer, Rudolph Research) under identical experimental conditions. A refractive index value of 1.35616 was used for the CP buffer, and 0.159 cm^3 g^{-1} and 0.129 cm^3 g^{-1} were used for dn/dc values for the ampetoids and $PMP1_{10}$, respectively.

OWLS was also used for *in situ* protein adsorption experiments; TiO_2-coated waveguide sensors were modified with the polymers as explained previously. After adequate equilibration of the sensors in HEPES buffer, human serum solution was injected and allowed to adsorb for 20 min at 37°C before rinsing with HEPES buffer. A refractive index value of 1.33127 was used for the HEPES buffer, and a standard value of 0.182 cm^3 g^{-1} was used for dn/dc in the protein-adsorption calculations (Pasche et al. 2003). Averages and SDs from three replicates are reported. Statistical significance was assessed using a one-way ANOVA and Tukey's *post hoc* test with 95% confidence intervals (SPSS, Chicago, IL).

ABT activity on surfaces

E. coli cells were streaked from frozen stocks onto Mueller–Hinton agar and incubated overnight at 37°C. A few colonies were then used to inoculate 25 ml of sterile Mueller–Hinton broth (MHB) and grown overnight at 37°C. TiO_2-coated glass slides were modified with the polymers using the previously described procedure. Two-well chambers were clamped to the slides and sealed by injecting silastic resin, which was allowed to cure overnight. Slides were sterilised by exposure to UV light for 10 min. The bacterial suspension was concentrated by centrifugation and resuspended in PBS at a concentration of 5×10^7 CFU ml^{-1}; 2 ml of the *E. coli* suspension was added to each slide chamber. Slide chamber was covered and placed in a humidified incubator at 37°C; after 2 h, nonadherent bacteria were removed by inverted centrifugation for 2 min at 30 rcf in sealed bags filled with PBS (Jensen et al. 2004). Adherent bacteria were stained with FITC (6 μg ml^{-1}) in PBS for 15 min at 37°C. FITC has been observed to only penetrate into cells with compromised membranes (Makovitzki et al. 2006). Slides were rinsed with PBS and imaged by confocal microscopy equipped with an inverted microscope (Leica TCS SP2). Phase contrast and fluorescent (488-nm band-pass filter for excitation of FITC) images were taken at identical locations to determine bacterial cell count and percent stained with FITC. The microscope images were quantified using

thresholding in ImageJ, and averages with SDs for at least nine images from one slide are reported. Although slides were prepared in duplicate or triplicate and consistency was qualitatively confirmed between experimental samples, the reported counts and images were obtained from a single slide for each condition.

Fibroblast adhesion assay

3T3-Swiss albino fibroblasts were maintained at 37°C and 5% CO_2 in Dulbecco's modified Eagle's medium (DMEM) containing 10% foetal bovine serum (FBS) and 100 U ml^{-1} of penicillin/streptomycin. Immediately before use, fibroblasts of passage 12–16 were harvested using 0.25% trypsin-EDTA, resuspended in DMEM with 10% FBS and counted using a haemacytometer. Modified and unmodified TiO_2 substrata were sterilised by exposure to UV light for 10 min; cells were seeded on each substratum at a density of 2.9×10^3 cells cm^{-2} and maintained in DMEM with FBS at 37°C and 5% CO_2 for 4 h, after which adherent cells were fixed in 3.7% paraformaldehyde for 5 min and stained with 5 μM 1,1′-dioctadecyl-3,3,3′,3′-tetramethylindocarbocyanine perchlorate (DiI) for epifluorescent microscope counting.

Quantitative cell attachment data were obtained by acquiring nine images (10× magnification) from random locations on each substratum using a Leica epifluorescent microscope (W. Nuhsbaum, McHenry, IL) equipped with a SPOT RT digital camera (Diagnostics Instruments, Sterling Heights, MI). Three identical substrata for each experiment were analysed, and the total projected cellular area was quantified using thresholding in Metamorph (Molecular Devices, Downingtown, PA); the mean and SD are reported. Statistical significance was assessed using a one-way ANOVA and Tukey's *post hoc* test with 95% confidence intervals (SPSS, Chicago, IL).

Results and discussion

AMB peptoid design

The AMB incorporated previously identified sequences that mimic helical AMB peptides (Patch and Barron 2003; Chongsiriwatana et al. 2008). PMP1-AMP contained an N-terminal 12-mer peptoid sequence composed of α-chiral aromatic (S)-*N*-(1-phenylethyl)-glycine (*N*spe), achiral cationic *N*-(4-aminobutyl)glycine (*N*Lys) and one proline residue, selected based on its reported low MIC and high selectivity ratio for bacterial cells over mammalian cells (Chongsiriwatana et al. 2008). PMP1-C contained a terminal 12-mer peptoid sequence composed of bulky α-chiral side-chains (S)-*N*-(*sec*-butyl)glycine (*N*ssb) and cationic *N*-(4-aminobutyl)glycine (*N*Lys) residues, selected as a control because this sequence exhibited very low ABT and hemolytic activity (Patch and Barron 2003). Both polymers were tethered to the substratum surface via a peptide/peptoid construct composed of adhesive peptides (DOPA, Lys) and AF peptoids (*N*me). The $(Nme)_{20}$-$(DOPA\text{-}Lys)_2$-DOPA construct (PMP1) was previously shown to adsorb strongly to TiO_2 substrata and provide excellent protein and cell fouling-resistant properties (Statz et al. 2005, 2008). A shorter version of this construct, $PMP1_{10}$, was synthesised in order to 'backfill' the surfaces with a passive AF peptoid after modification with PMP1-AMP. The polymers were purified using RP-HPLC, and the purity and molecular weight of the resulting fractions were determined using RP-HPLC and MALDI-MS (Figures S1 and S2). The chemical structures of PMP1-AMP, PMP1-C and $PMP1_{10}$ are shown in Figure 1.

AMB activity – solution assay

The polymers were initially tested to determine their ABT properties in the solution state. The ABT activities of the compounds were tested using the methods described above for both Gram-negative and Gram-positive bacterial strains. The MICs are reported in Table 1. Although PMP1-AMP was active against all bacterial strains, the MIC was 2–4 times greater than that for AMP alone; this increase can likely be explained by the presence of the additional 26 residues contained in the *N*me tether and adhesive anchor portion of the polymer. As expected, peptoid C, PMP1-C and $PMP1_{10}$ were not active at the tested concentrations. Although MIC values are useful predictors for AMBs in solution, these measurements do not directly correlate to the amount required for surface-immobilised applications because interactions between the bacteria and the immobilised polypeptoids are expected to differ from the interactions when the ampetoids are free in solution.

The effects of the additional peptide and peptoid residues on the secondary structure of AMP were

Table 1. Antibacterial activities (MICs) of the ampetoids and polymer components with *E. coli*, *B. subtilis*, *S. epidermidis* and *P. aeruginosa*.

	MIC (μM)			
	E. coli	*B. subtilis*	*S. epidermidis*	*P. aeruginosa*
PMP1-AMP	50	3.1	3.1	200
AMP	12.5	1.6	1.6	25
PMP1-C	>100	>100	>100	>100
Peptoid C	>100	>100	>100	>100
PMP1	>100	>100	>100	>100

investigated by measuring the overall helix structure of the polymers using CD spectroscopy (Figure S3). PMP1-AMP and AMP exhibited similar spectral features, indicating the presence of a defined helical structure as was shown previously for AMP (Chongsiriwatana et al. 2008). The helical structures of PMP1-AMP and AMP are due to the incorporation of bulky α-chiral side chains which cause steric constraints (Armand et al. 1998; Wu et al. 2001, 2003; Sanborn et al. 2002). Peptoid C, PMP1-C and $PMP1_{10}$ did not have helical structures.

Surface characterisation

Next, adsorption of the polymers onto TiO_2 substrata was investigated using OWLS and XPS. In order to create surfaces with both active ABT and passive AF properties, surfaces were modified with PMP1-AMP or PMP1-C, first, and then backfilled with the shorter $PMP1_{10}$. Modifying surfaces with a two-step approach involving grafting of a longer polymer followed by backfilling with a shorter one, has been shown to be an effective strategy for enhancing the AF performance of polymer brushes (Fang et al. 2005; Satomi et al. 2007; Uchida et al. 2007). In the present case, backfilling with $PMP1_{10}$ should facilitate extension of the active AMP moiety away from the surface for interaction with bacteria that encounter the modified surface. Like AMB peptides, ampetoids must interact with the bacterial membranes (Pag et al. 2004; Hancock and Sahl 2006; Jenssen et al. 2006); therefore, the mobility of the longer ampetoid chains would be expected to be important for AB activity. Gabriel et al. (2006) demonstrated that PEG spacers were necessary when immobilising cathelin LL37 on titanium surfaces because lateral mobility of surface-bound AMPs and parallel orientation of the peptide helices are required for interaction of the peptides with bacterial membranes.

Optimum modification conditions were determined by conducting OWLS experiments; PMP1-AMP was adsorbed onto TiO_2 waveguides using various concentrations and modification conditions. The goal was to adsorb a sub-monolayer coating of the polymer onto the surface. Subsequently, $PMP1_{10}$ was adsorbed on the waveguide containing the PMP1-AMP layer in order to backfill between the ampetoid chains with this AF polymer. Although the $PMP1_{10}$ may be able to adsorb on top of the PMP1-AMP layer, most likely the $PMP1_{10}$ will adsorb to any remaining exposed areas of the TiO_2 waveguide due to the strong interactive forces between DOPA and metal oxides (Statz et al. 2005; Lee et al. 2006). The OWLS mass plot, shown in Figure 2a, represents the optimum conditions for two-stage adsorption: 2 h adsorption of a 0.5 mg ml^{-1} solution of PMP1-AMP in H_2O, followed by 6-h adsorption of a 1.0 mg ml^{-1} solution of $PMP1_{10}$ in CP buffer. The resulting adsorbed masses correlate to a polymer coating composed of ~40% PMP1-AMP AB polymer and 60% of $PMP1_{10}$ AF polymer. The experiments were repeated using identical adsorption conditions for PMP1-C, shown in Figure 2b, yielding a surface composed of ~43% ABT polymer and 57% AF polymer. These conditions were selected for preparation of mixed surfaces in all subsequent experiments.

The elemental compositions of the polymer layers are reported in Table 2, derived from the XPS survey scan spectra shown in Figure S4. C, N and O signals are representative of the peptide/peptoid backbone and side-chains of the polymers. Ti signal was detected for all samples from the underlying TiO_2 substrata. The decrease in Ti signal for $PMP1_{10}$-modified substrata indicates successful modification, and the further decrease in Ti % for the PMP1-AMP and PMP1-C surfaces backfilled with $PMP1_{10}$ suggests that the polymer coating becomes thicker during the backfilling step. The detected F signal is from the single

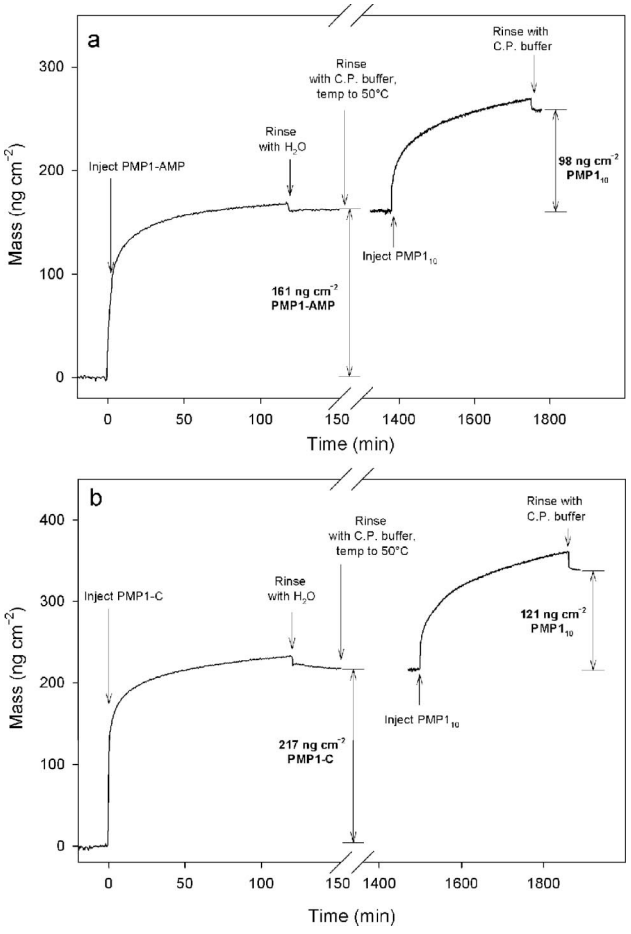

Figure 2. OWLS plot of mass adsorption for PMP1-AMP and $PMP1_{10}$ (a) and PMP1-C and $PMP1_{10}$ (b).

Table 2. Atomic compositions of bare and modified TiO_2 substrata as determined from high-resolution XPS spectra.

	Experimental composition (atom %)				
Substrata	C	N	O	F	Ti
TiO_2	16.8	0.2	54.8	0.0	28.2
$PMP1_{10}$ only	48.5	6.9	34.8	0.0	9.8
PMP1-AMP*	54.1	8.3	29.5	0.2	7.9
PMP1-C*	52.8	7.3	32.0	0.2	7.7

*Back-filled with $PMP1_{10}$.

trifluoroethyl glycine residue included in the PMP1-AMP and PMP1-C polymers; the presence of the F signal after backfilling indicates that PMP1-AMP and PMP1-C remained on the surface after backfilling with $PMP1_{10}$.

ABT activity – substrata

Bacterial experiments on modified TiO_2 slides were performed by exposing the surfaces to an *E. coli* suspension for 2 h and then centrifuging to remove unattached and weakly attached bacterial cells. The bacteria remaining on the surfaces were imaged in phase contrast for determination of cell numbers, and in fluorescence after staining with FITC to detect cells with compromised membranes. Images of representative areas of the substrata are shown in Figure 3. From these images, the total numbers of adherent bacteria (from phase contrast) and the percentage of attached cells with compromised membranes (from FITC staining) were determined, and are shown in Table 3.

E. coli attachment to TiO_2 was reduced upon modification with $PMP1_{10}$, which is in general agreement with a previous study on attachment of *S. epidermidis* and *E. coli* to TiO_2 modified with a 20-mer *N*me peptoid (Statz et al. 2008). The number of *E. coli* attached to PMP1-AMP was comparable with that on bare TiO_2 surfaces, whereas attachment to PMP1-C was much higher than on PMP1-AMP and TiO_2 surfaces. Compared with $PMP1_{10}$, increased bacterial attachment to PMP1-AMP and PMP1-C surfaces could be explained either by direct interaction of the N-terminal peptoid sequences with the bacterial cell membrane, or through attachment of the bacteria to an adsorbed protein layer. In the case of PMP1-C, the terminal peptoid is unlikely to be membrane-active because this construct has no ABT properties in solution, suggesting a role for protein adsorption. With this in mind, protein adsorption to $PMP1_{10}$, and PMP1-AMP and PMP1-C backfilled with $PMP1_{10}$ was determined. The results shown in Table 4 indicate that, although serum protein adsorption was increased on PMP1-AMP and PMP1-C substrata compared with $PMP1_{10}$ only substrata, the adsorbed masses were significantly lower than on unmodified TiO_2 sensors ($p < 0.05$). That the peptoid

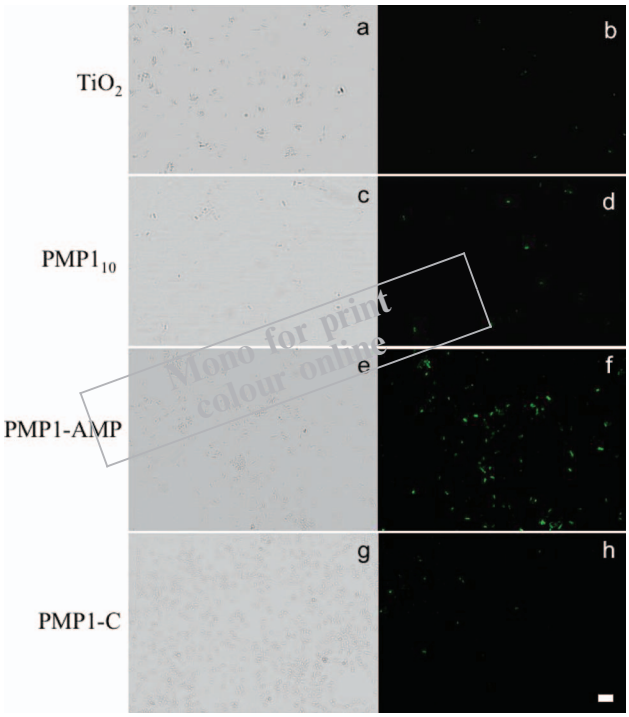

Figure 3. Confocal microscopy images (phase contrast images on left and fluorescent images on right) for *E. coli* after 2 h incubation on bare TiO_2 (a and b), $PMP1_{10}$ (c and d), PMP1-AMP (e and f), and PMP1-C (g and h) modified substrata. Scale bar = 10 μm.

Table 3. Quantification of bacterial adhesion and membrane permeation on bare and modified TiO_2 substrata.

Substrata	Total cell count (cells cm^{-2})	% FITC-stained
TiO_2	74 ± 31	5 ± 3
$PMP1_{10}$ only	20 ± 7	27 ± 15
PMP1-AMP*	87 ± 13	69 ± 25
PMP1-C*	189 ± 82	4 ± 3

Note: SDs from the mean for nine images are reported.
*Back-filled with $PMP1_{10}$.

Table 4. Quantification of short-term (20 min) human serum protein adsorption on bare and modified TiO_2 sensors using OWLS.

Substratum	Adsorbed serum mass (ng cm^{-2})
Bare TiO_2	342 ± 21
$PMP1_{10}$	51 ± 7
PMP1-AMP*	119 ± 40
PMP1-C*	88 ± 30

Note: SDs from the mean for three replicates are reported.
*Back-filled with $PMP1_{10}$.

side-chains of the *N*-terminal segments of PMP1-AMP and PMP1-C increase fouling by macromolecules is not surprising given the hydrophobic nature of the *N*spe and *N*ssb residues in these sequences (Ostuni et al. 2001).

Staining of adhered *E. coli* with FITC revealed that the highest percentage of bacterial cells with compromised membranes occurred on the active PMP1-AMP polymer surface when compared with PMP1-C, $PMP1_{10}$ only and TiO_2 surfaces (Table 3). Although the percentage death on the $PMP1_{10}$ substrata was surprisingly high, overall cell adhesion was much lower than on the PMP1-AMP substrata. Therefore, the total number of FITC-stained bacteria on the active surface was $>10\times$ greater than on the $PMP1_{10}$ surfaces. The percentage of FITC-stained bacteria on the PMP1-C substrata was low and comparable with the control TiO_2 substrata, indicating no ABT effects from this peptoid. Although ABT activity was only demonstrated for *E. coli*, similar results would be expected for *B. subtilis, S. epidermidis* and *P. aeruginosa*, based on the MIC values determined for the ampetoids in solution (Table 1).

AF properties of substrata-mammalian cells

To further assess the AF properties of these substrata, a short-term fibroblast adhesion assay was conducted, the results of which are shown in Figure 4. Although the total projected area of adherent cells was greater on the polymer-modified surfaces containing the ampetoids than on the $PMP1_{10}$ substrata, all modified substrata had a significant reduction ($p < 0.05$) in cell adhesion compared with the bare TiO_2 substrata. The adherent cells appeared to be less spread on the ampetoid surfaces than on the bare TiO_2 substrata, suggesting that, although the fibroblasts may be able to weakly attach, they are not capable of spreading on the surface. These fibroblast adhesion results are consistent with the relative levels of serum protein adsorption (Table 4), suggesting that the modestly higher cell adhesion on the ampetoid-containing surfaces can be explained by the higher adsorbed protein on these surfaces.

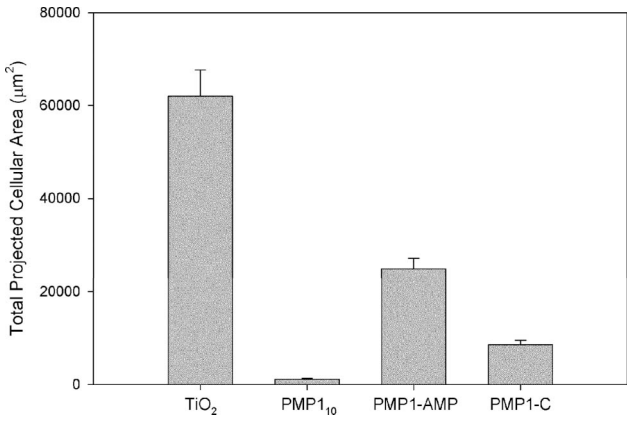

Figure 4. Total projected cellular area for 4 h 3T3 fibroblast adhesion assay on bare TiO_2 and modified TiO_2 substrata.

Conclusions

In summary, peptoids are promising alternatives to conventional AMBs because of their stability, ease of synthesis and low cytotoxicity. The results shown here suggest that peptoid mimics of AMB peptides can be immobilised onto surfaces, rendering these surfaces capable of compromising the membranes of attached bacteria. The ABT activity of the ampetoids was initially demonstrated in solution-based assays, and subsequently shown for *E coli* when immobilised onto surfaces. Substrata modified with PMP1-AMP exhibited increased bacterial adhesion, and a significant percentage of the adherent bacteria had compromised membranes, indicating that the surface-immobilised ampetoids were capable of interacting with the bacteria. By modifying the surfaces with both the ampetoids and $PMP1_{10}$, the passive resistance to protein and mammalian cell fouling was improved compared with bare TiO_2, although maintaining sufficient ampetoid concentration for ABT activity. It remains to be seen whether the benefits of having an active ABT component on the surface may outweigh the disadvantages of slightly increased bacterial adhesion. More detailed future studies involving fine-tuning the ratio of adsorbed passive and active components, or the composition of the active component, may reveal a surface composition that combines even greater resistance to protein and bacterial adhesion with an ABT effect. For some medical device applications, more sophisticated designs incorporating hydrolytic or enzymatic cleavage sites within the PMP1-AMP backbone might allow for cleavage of the ABT domain from the coating once the risk of post-operative infection had passed, leaving behind a protein and cell resistant PMP1 coating.

Acknowledgements

This research was supported by NIH grants R37 DE014193 (PBM), R01 AI072666 and R01 EB003806 (AEB). XPS surface analysis was performed at KeckII/NUANCE, and confocal microscopy was performed at the Biological Imaging Facility at Northwestern University.

References

Appendini P, Hotchkiss JH. 2001. Surface modification of poly(styrene) by the attachment of an antimicrobial peptide. J Appl Polym Sci. 81:609–616.

Armand P, Kirshenbaum K, Goldsmith RA, Farr-Jones S, Barron AE, Truong KTV, Dill KA, Mierke DF, Cohen FE, Zuckermann RN, et al. 1998. NMR determination of the major solution conformation of a peptoid pentamer with chiral side chains. Proc Natl Acad Sci USA. 95:4309–4314.

Aumsuwan N, Heinhorst S, Urban MW. 2007. Antibacterial surfaces on expanded polytetrafluoroethylene; *Penicillin* attachment. Biomacromolecules. 8:713–718.

Cen L, Neoh KG, Ying L, Kang ET. 2004. Surface modification of polymeric films and membranes to achieve antibacterial properties. Surf Interface Anal. 36:716–719.

Chapman RG, Ostuni E, Liang MN, Meluleni G, Kim E, Yan L, Pier G, Warren HS, Whitesides GM. 2001. Polymeric thin films that resist the adsorption of proteins and the adhesion of bacteria. Langmuir. 17:1225–1233.

Cheng Z, Zhu X, Shi ZL, Neoh KG, Kang ET. 2005. Polymer microspheres with permanent antibacterial surface from surface-initiated atom transfer radical polymerization. Ind Eng Chem Res. 44:7098–7104.

Chongsiriwatana NP, Patch JA, Czyzewski AM, Dohm MT, Ivankin A, Gidalevitz D, Zuckermann RN, Barron AE. 2008. Peptoids that mimic the structure, function, and mechanism of helical antimicrobial peptides. Proc Natl Acad Science USA. 105:2794–2799.

Costerton JW, Stewart PS, Greenberg EP. 1999. Bacterial biofilms: a common cause of persistent infections. Science. 284:1318–1322.

de Feijter JA, Benjamins J, Veer FA. 1978. Ellipsometry as a tool to study adsorption behavior of synthetic and biopolymers at air–water-interface. Biopolymers. 17: 1759–1772.

Fang F, Satulovsky J, Szleifer I. 2005. Kinetics of protein adsorption and desorption on surfaces with Grafted Polymers. Biophys J. 89:1516–1533.

Fu J, Ji J, Yuan W, Shen J. 2005. Construction of anti-adhesive and antibacterial multilayer films via layer-by-layer assembly of heparin and chitosan. Biomaterials. 26:6684–6692.

Gabriel M, Nazmi K, Veerman EC, NieuwAmerongen AV, Zentner A. 2006. Preparation of LL-37-grafted titanium surfaces with bactericidal activity. Bioconjugate Chem. 17:548–550.

Habash M, Reid G. 1999. Microbial biofilms: their development and significance for medical device-related infections. J Clin Pharmacol. 39:887–898.

Hancock REW, Sahl H-G. 2006. Antimicrobial and host-defense peptides as new anti-infective therapeutic strategies. Nat Biotech. 24:1551–1557.

Harbers GM, Emoto K, Greef C, Metzger SW, Woodward HN, Mascali JJ, Grainger DW, Lochhead MJ. 2007. Functionalized poly(ethylene glycol)-based bioassay surface chemistry that facilitates bio-immobilization and inhibits nonspecific protein, bacterial, and mammalian cell adhesion. Chem Mater. 19:4405–4414.

Huh MW, Kang I-K, Lee DH, Kim WS, Lee DH, Park LS, Min KE, Seo KH. 2001. Surface characterization and antibacterial activity of chitosan-grafted poly(ethylene terephthalate) prepared by plasma glow discharge. J Appl Polym Sci. 81:2769–2778.

Jensen TW, Hu BH, Delatore SM, Garcia AS, Messersmith PB, Miller WM. 2004. Lipopeptides incorporated into supported phospholipid monolayers have high specific activity at low incorporation levels. J Am Chem Soc. 126:15223–15230.

Jenssen H, Hamill P, Hancock REW. 2006. Peptide antimicrobial agents. Clin Microbiol Rev. 19:491–511.

Jose B, Antoci V, Jr., Zeiger AR, Wickstrom E, Hickok NJ. 2005. Vancomycin covalently bonded to titanium beads kills *Staphylococcus aureus*. Chem Biol. 12:1041–1048.

Kenawy E-R, Worley SD, Broughton R. 2007. The chemistry and applications of antimicrobial polymers: a state-of-the-art review. Biomacromolecules. 8:1359–1384.

Kingshott P, Wei J, Bagge-Ravn D, Gadegaard N, Gram L. 2003. Covalent attachment of poly(ethylene glycol) to surfaces, critical for reducing bacterial adhesion. Langmuir. 19:6912–6921.

Krapcho AP, Kuell CS. 1990. Mono-protected diamines. *N-tert*-butoxycarbonyl-α,ω-alkanediamines from α,ω-alkanediamines. Synth Comm. 20:2559–2564.

Krishnan S, Ward RJ, Hexemer A, Sohn KE, Lee KL, Angert ER, Fischer DA, Kramer EJ, Ober CK. 2006. Surfaces of fluorinated pyridinium block copolymers with enhanced antibacterial activity. Langmuir. 22:11255–11266.

Lee H, Scherer NF, Messersmith PB. 2006. Single-molecule mechanics of mussel adhesion. Proc Natl Acad Sci USA. 103:12999–13003.

Lee SB, Koepsel RR, Morley SW, Matyjaszewski K, Sun Y, Russell AJ. 2004. Permanent, nonleaching antibacterial surfaces: Part 1: synthesis by atom transfer radical polymerization. Biomacromolecules. 5:877–882.

Makovitzki A, Avrahami D, Shai Y. 2006. Ultrashort antibacterial and antifungal lipopeptides. Proc Natl Acad Sci USA. 103:15997–16002.

Marini M, De Niederhausern S, Iseppi R, Bondi M, Sabia C, Toselli M, Pilati F. 2007. Antibacterial activity of plastics coated with silver-doped organic-inorganic hybrid coatings prepared by sol–gel processes. Biomacromolecules. 8:1246–1254.

Miller SM, Simon RJ, Ng S, Zuckermann RN, Kerr JM, Moos WH. 1995. Comparison of the proteolytic susceptibilities of homologous L-amino acid, D-amino acid, and *N*-substituted glycine peptide and peptoid oligomers. Drug Dev Res. 35:20–32.

Murata H, Koepsel RR, Matyjaszewski K, Russell AJ. 2007. Permanent, non-leaching antibacterial surfaces-2: how high density cationic surfaces kill bacterial cells. Biomaterials. 28:4870–4879.

Ostuni E, Chapman RG, Holmlin RE, Takayama S, Whitesides GM. 2001. A survey of structure–property relationships of surfaces that resist the adsorption of protein. Langmuir. 17:5605–5620.

Pag U, Oedenkoven M, Papo N, Oren Z, Shai Y, Sahl HG. 2004. *In vitro* activity and mode of action of diastereomeric antimicrobial peptides against bacterial clinical isolates. J Antimicrob Chemother. 53:230–239.

Pasche S, De Paul SM, Voros J, Spencer ND, Textor M. 2003. Poly(L-lysine)-*graft*-poly(ethylene glycol) assembled monolayers on niobium oxide surfaces: a quantitative study of the influence of polymer interfacial architecture on resistance to protein adsorption by ToF-SIMS and *in situ* OWLS. Langmuir. 19:9216–9225.

Patch JA, Barron AE. 2003. Helical peptoid mimics of magainin − 2 amide. J Am Chem Soc. 125:12092–12093.

Porter EA, Weisblum B, Gellman SH. 2002. Mimicry of host-defense peptides by unnatural oligomers: antimicrobial beta-peptides. J Am Chem Soc. 124:7324–7330.

Ramstedt M, Houriet R, Mossialos D, Dieter H, Mathieu HJ. 2007a. Wet chemical silver treatment of endotracheal tubes to produce antibacterial surfaces. J Biomed Mater Res Part B: Appl Biomat. 83B:169–180.

Ramstedt M, Cheng N, Azzaroni O, Mossialos D, Mathieu HJ, Huck WT. 2007b. Synthesis and characterization of poly(3-sulfopropylmethacrylate) brushes for potential antibacterial applications. Langmuir. 23:3314–3321.

Sambhy V, MacBride MM, Peterson BR, Sen A. 2006. Silver bromide nanoparticle/polymer composites: dual action tunable antimicrobial materials. J Am Chem Soc. 128:9798–9808.

Sanborn TJ, Wu CW, Zuckerman RN, Barron AE. 2002. Extreme stability of helices formed by water-soluble poly-*N*-substituted glycines (polypeptoids) with alpha-chiral side chains. Biopolymers. 63:12–20.

Satomi T, Nagasaki Y, Kobayashi H, Otsuka H, Kataoka K. 2007. Density control of poly(ethylene glycol) layer to regulate cellular attachment. Langmuir. 23:6698–6703.

Statz AR, Barron AE, Messersmith PB. 2008. Protein, cell and bacterial fouling resistance of polypeptoid-modified surfaces: effect of side-chain chemistry. Soft Mater. 4:131–139.

Statz AR, Meagher RJ, Barron AE, Messersmith PB. 2005. New peptidomimetic polymers for antifouling surfaces. J Am Chem Soc. 127:7972–7973.

Tiller JC, Liao CJ, Lewis K, Klibanov AM. 2001. Designing surfaces that kill bacteria on contact. Proc Natl Acad Sci USA. 98:5981–5985.

Tiller JC, Lee SB, Lewis K, Klibanov AM. 2002. Polymer surfaces derivatized with poly(vinyl-*N*-hexylpyridinium) kill airborne and waterborne bacteria. Biotechnol Bioeng. 79:465–471.

Uchida K, Hoshino Y, Tamura A, Yoshimoto K, Kojima S, Yamashita K, Yamanaka I, Otsuka H, Kataoka K, Nagasaki Y. 2007. Creation of a mixed poly(ethylene glycol) tethered-chain surface for preventing the non-specific adsorption of proteins and peptides. Biointerphases. 2:126–130.

Voros J, Ramsden JJ, Csucs G, Szendro I, De Paul SM, Textor M, Spencer ND. 2002. Optical grating coupler biosensors. Biomaterials. 23:3699–3710.

Wu CW, Sanborn TJ, Huang K, Zuckermann RN, Barron A. 2001. Peptoid oligomers with a-chiral, aromatic side chains: sequence requirements for the formation of stable peptoid helices. J Am Chem Soc. 123:6778–6784.

Wu CW, Kirshenbaum K, Sanborn TJ, Patch JA, Huang K, Dill KA, Zuckermann RN, Barron AE. 2003. Structural and spectroscopic studies of peptoid oligomers with alpha-chiral aliphatic side chains. J Am Chem Soc. 125:13525–13530.

Zuckermann RN, Kerr JM, Kent SBH, Moos WH. 1992. Efficient method for the preparation of peptoids [oligo(*N*-substituted glycines)] by submonomer solid-phase synthesis. J Am Chem Soc. 114:10646–10647.